

Estimating gas accretion in disc galaxies using the Kennicutt-Schmidt law

Filippo Fraternali^{1,2*} and Matteo Tomassetti^{1,3,4†}

¹*Astronomy Department, University of Bologna, via Ranzani 1, 40127, Bologna (IT)*

²*Kapteyn Astronomical Institute, Postbus 800, 9700 AV, Groningen (NL)*

³*Argelander Institut für Astronomie, University of Bonn, Auf dem Hügel 71, 53121, Bonn (D)*

⁴*Max Planck Institut für Radioastronomie, Auf dem Hügel 69, 53121, Bonn (D)*

Accepted 2012 Month day. Received 2012 Month day

ABSTRACT

We show how the existence of a relation between the star formation rate and the gas density, i.e. the Kennicutt-Schmidt law, implies a continuous accretion of fresh gas from the environment into the discs of spiral galaxies. We present a method to derive the gas infall rate in a galaxy disc as a function of time and radius, and we apply it to the disc of the Milky Way and 21 galaxies from the THINGS sample. For the Milky Way, we found that the ratio between the past and current star formation rates is about 2 – 3, averaged over the disc, but it varies substantially with radius. In the other disc galaxies there is a clear dependency of this ratio with galaxy stellar mass and Hubble type, with more constant star formation histories for small galaxies of later type. The gas accretion rate follows very closely the SFR for every galaxy and it dominates the evolution of these systems. The Milky Way has formed two thirds of its stars after $z = 1$, whilst the mass of cold gas in the disc has remained fairly constant with time. In general, all discs have accreted a significant fraction of their gas after $z = 1$. Accretion moves from the inner regions of the disc to the outer parts, and as a consequence star formation moves inside-out as well. At $z = 0$ the peak of gas accretion in the Galaxy is at about 6 – 7 kpc from the centre.

Key words: Galaxy: evolution – galaxies: star formation – galaxies: ISM – galaxies: evolution

1 INTRODUCTION

Star formation is the fundamental process that shapes galaxies into different classes. Although the majority of stars in the local Universe are found in spheroidal systems, most of the star formation is contributed by disc galaxies of the later types (beyond Sb). The key ingredient for star formation is cold (*star-forming*) gas, which is present almost exclusively in disc galaxies. However, the amount of cold gas currently available in galaxy discs appears rather scant. Kennicutt (1998b) estimated that disc galaxies have current star formation rates ranging from a few to about $\simeq 10 M_{\odot} \text{yr}^{-1}$. Thus, considering a typical gaseous mass of a few $10^9 M_{\odot}$, the gas consumption time scale (i.e. the time needed to exhaust the gas fuel with a constant star formation rate) is always of the order of a few Gigayears. This result, known as the gas-consumption dilemma (Kennicutt 1983), suggests

the need for continuous accretion of cold gas onto galaxy discs (e.g. Sancisi et al. 2008).

Several pieces of evidence show that disc galaxies should collect fresh gas from the environment in order to sustain their star formation. In the Milky Way, the star formation rate (SFR) in the solar neighbourhood appears to have remained rather constant in the last ~ 10 Gyr (e.g. Twarog 1980; Rocha-Pinto et al. 2000; Binney et al. 2000), suggesting a continuous replenishment of the gas supply. Simple (closed-box) models of chemical evolution for our Galaxy predict too few metal deficient *G-dwarf* stars than observed (Searle & Sargent 1972; Pagel & Patchett 1975; Haywood 2001). These observations are easily explained by accounting for infall of fresh unpolluted gas (e.g. Chiappini et al. 1997, 2001). Observations of Damped Lyman Alpha systems show almost no evolution in the neutral gas content of structures in the Universe (Zwaan et al. 2005; Lah et al. 2007; Jorgenson et al. 2009). Hopkins et al. (2008) pointed out that this constancy of gas density can be explained assuming a rate

* E-mail: filippo.fraternali@unibo.it

† E-mail: mtomas@astro.uni-bonn.de

of gas replenishment proportional to the universal SFR density. Bauermeister et al. (2010) converged to a similar result when comparing the evolution of the molecular gas depletion rate with that of the cosmic star formation history (SFH). Finally, the derivations of SFHs for galaxies with different stellar masses consistently show that late type systems do have a rather constant SFR throughout the whole Hubble time (e.g. Panter et al. 2007). These findings, other than being the signature of *downsizing* in cosmic structures, point at a continuous infall of gas onto galaxies of late Hubble types.

The way gas accretion into galaxies takes place is still a matter of debate. The classical picture states that thermal instabilities should cause the cooling of the hot coronae that surround disc galaxies and be the source of cold gas infall (e.g. Maller & Bullock 2004; Kaufmann et al. 2006). However, recent studies have shown that, due to a combination of buoyancy and thermal conduction, hot coronae turn out to be remarkably stable and thermal instability does not appear to be a viable mechanism for gas accretion (Binney et al. 2009; Joung et al. 2011). On the other hand, accretion may take place in the form of cold flows but the importance of this process is expected to drop significantly for redshift $z < 2$ (Dekel & Birnboim 2006; van de Voort et al. 2011). Observations of local gas accretion at 21-cm emission seem to show too little gas around galaxies in the form of HI (high-velocity) clouds to justify an efficient feeding of the disc star formation (Sancisi et al. 2008; Thom et al. 2008; Fraternali 2009). However, UV absorption towards quasars and halo stars point to the possibility that ionised gas at temperatures between a few 10^4 and a few 10^5 K could fill the gap between expectations and data (Bland-Hawthorn 2009; Collins et al. 2009; Lehner & Howk 2011).

In this paper, we estimate gas accretion in galactic discs indirectly by comparing basic physical properties of galaxies today. Our model relies on the existence of a law relating the star formation rate density (SFRD) and the gas surface density (Σ_{gas}) holding at every redshift, i.e. the Kennicutt-Schmidt (K-S) law (Schmidt 1959; Kennicutt 1998b). This approach has similarities with the model of Naab & Ostriker (2006) that we describe in detail in Section 4. The paper is organized as follows. Section 2 describes our method. In Section 3 we apply our model to the Milky Way disc and to a sample of external discs. In Section 4 we discuss our results. Section 5 sums up.

2 DESCRIPTION OF THE MODEL

The evolution of gas and stellar densities (Σ_{gas} and Σ_*) in a galactic disc as a function of the lookback time t is described by the following equations (Tinsley 1980):

$$-\frac{d\Sigma_*}{dt} = +\text{SFRD} - \dot{\Sigma}_{\text{fb}} \quad (1)$$

$$-\frac{d\Sigma_{\text{gas}}}{dt} = -\text{SFRD} + \dot{\Sigma}_{\text{fb}} + \dot{\Sigma}_{\text{ext}} \quad (2)$$

where SFRD is the star formation rate density, $\dot{\Sigma}_{\text{fb}}$ is the contribution from stellar feedback and $\dot{\Sigma}_{\text{ext}}$ is the inflow/outflow rate from/to the external environment. SFRD gives the rate at which stars are formed or, with a sign inversion, the rate at which gas is consumed, whilst $\dot{\Sigma}_{\text{fb}}$ represents the gas density per unit time returned by stellar

evolution to the gas reservoir in the disc. We treat the stellar feedback with the instantaneous recycling approximation (I.R.A.), meaning that the fractional mass that stars return to the ISM at each time is assumed to be constant and equal to the return factor \mathcal{R} . Equations (1)-(2) modify as follows:

$$-\frac{d\Sigma_*}{dt} = (1 - \mathcal{R})\text{SFRD} \quad (3)$$

$$-\frac{d\Sigma_{\text{gas}}}{dt} = -(1 - \mathcal{R})\text{SFRD} + \dot{\Sigma}_{\text{ext}} \quad (4)$$

In Section 4.1 we discuss the effect of a delayed return.

The parameter \mathcal{R} in eqs. (3)-(4) depends on the IMF and the fraction $\eta(M)$ of mass that a star of mass M returns to the ISM, called the *stellar initial versus final mass relation*. Following the prescription of Kennicutt et al. (1994) we assume that high-mass stars ($M > 8 M_\odot$) all leave a $1.4 M_\odot$ remnant. Low-mass stars are assumed to leave remnants with masses between ~ 0.5 and $\sim 1.3 M_\odot$, with a linear dependency from the initial mass (see Chapter 2 of Matteucci, F. 2001, for details). Assuming a Salpeter IMF, our fiducial value for the recycling parameter is $\mathcal{R} \simeq 0.30$. Assuming Kroupa (Kroupa et al. 1993) or Chabrier (Chabrier 2003) IMFs would make little difference, giving $\mathcal{R} = 0.31$ and $\mathcal{R} = 0.32$ (or $\mathcal{R} = 0.46$ for a flatter high-mass slope) respectively. With this value the gas consumption timescales are extended by a factor $(1 - \mathcal{R})^{-1} = 1.4$ (see Kennicutt et al. 1994).

The third term on the RHS of eq. (2) is the inflow/outflow term. The combination of eqs. (1) and (2) leads to an expression for this term:

$$\dot{\Sigma}_{\text{ext}} = -\frac{d\Sigma_*}{dt} - \frac{d\Sigma_{\text{gas}}}{dt} \quad (5)$$

In the following we often refer to this term as the accretion (or infall) rate.

Equations (1) and (2) can be applied to a galactic disc assuming that they are valid at each radius, i.e. that the disc can be divided into annuli that evolve independently. This assumption is equivalent to say that stars that form at a certain radius remain at that radius for the lifetime of the galactic disc. In Section 4.3 we discuss the effect of stellar migration and show that our main results do not change significantly. As a consequence of this assumption we can integrate eq. (1) from t_{form} (the lookback time at the disc formation) to $t = 0$ to get the current stellar surface density.

Clearly, in order to solve the above system one needs the SFRD as a function of lookback time and radius, i.e. the SFH as a function of radius. In the Milky Way, the SFH is known with fairly good precision only in the Solar Neighborhood (e.g. Rocha-Pinto et al. 2000; Cignoni et al. 2006). In external galaxies there have been pioneering attempts to estimate the SFH as a function of galactic radius (e.g. Gogarten et al. 2009; Weisz et al. 2011). In general, however, a precise determination of SFH(R) is beyond the capability of the current data. Therefore, for the time being, we must content ourselves with using simple parametrisations for the shape of the SFH. In the following section we describe how we estimate the trend of the SFH at each radius in a galactic disc. We consider only the disc, leaving aside the bulge/bar, which may have formed and evolved differently as it shows a markedly different SFH (e.g. Hopkins et al. 2001).

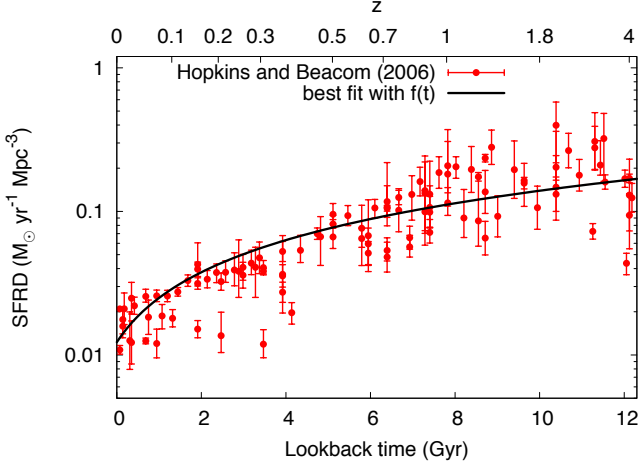


Figure 1. Evolution of the average SFR density of the Universe, the points are taken from Hopkins & Beacom (2006). The thick black curve shows a fit with our function $f(t)$ described in the text.

2.1 Reconstructing the SFH of a galaxy disc

We assume that the SFH in a galaxy disc can be described by a dimensionless and positive function $f = f(R, t)$. This allows us to write the star formation rate density as:

$$\text{SFRD}(R, t) = \text{SFRD}(R, 0) \times f(R, t) \quad (6)$$

where $\text{SFRD}(R, 0)$ is the radial distribution of the current star formation rate density, which we derive from the data. The simplest expression for f one can assume is a first order polynomial with time:

$$f_1(R, t) = 1 + [\gamma(R) - 1] \frac{t}{t_{\text{form}}} \quad (t_{\text{form}} \geq t \geq 0) \quad (7)$$

where t is the lookback time and t_{form} is the age of the stellar disc. With this definition, $\gamma(R)$ is the value of the function f at $t = t_{\text{form}}$ and sets the steepness of the SFH. A value of $\gamma(R)$ equal to unity represents a constant SFR over the disc lifetime, $\gamma(R) > (<)1$ describes a SFR that increases (decreases) with increasing lookback time.¹ The dependence of γ on the radius R allows us to describe different shapes of SFH within the disc. In Section 4.2 we discuss the effect of taking different forms for f , we anticipate that our main results remain unchanged.

We define the *global* γ for a galactic disc as:

$$\gamma = \frac{2\pi \int_0^{R_m} R \gamma(R) \text{SFRD}(R, 0) dR}{2\pi \int_0^{R_m} R \text{SFRD}(R, 0) dR} \quad (8)$$

where the integration is performed out to the maximum radius R_m ; the denominator is just the current SFR of the disc. This definition allows us to write an expression for the global SFR analogous to eqs. (6) and (7),

$$\text{SFR}(t) = \text{SFR}(0) \times \left[1 + (\gamma - 1) \frac{t}{t_{\text{form}}} \right] \quad (9)$$

As an illustration of the meaning of our parameter γ in

Fig. 1 we fit the average SFR density of the Universe with eq. (9). The data points are taken from Hopkins & Beacom (2006). Here we take $t_{\text{form}} = 12$ Gyr. For the other parameters we infer $\text{SFR}(0) = 0.012 \text{M}_{\odot} \text{yr}^{-1} \text{Mpc}^{-3}$ and $\gamma = 13.4$ as the best-fit values. This fit shows that the SFR density of the Universe as a whole is described by a value of γ much larger than unity, as expected given that the SFR density in the past was much higher than now. The shape of the universal SFR density is produced by the combined contribution of galaxies with very different SFHs. Massive red-sequence galaxies dominate the overall SFR at high- z , whilst late-type galaxies become relatively more and more important as time passes (e.g. Panter et al. 2007; Vincoletto et al. 2012). Although our parametrisation is only suitable for galaxies with non-negligible current SFR, taking γ as the ratio of $\text{SFR}(t_{\text{form}})/\text{SFR}(0)$, clearly red sequence galaxies must have $\gamma \gg 1$.

The above assumptions for the SFRD (eqs. 6 and 7) allow us to integrate eq. (3) from t_{form} to 0 to obtain:

$$\gamma(R) = \frac{2 \Sigma_*(R, 0)}{(1 - \mathcal{R}) t_{\text{form}} \text{SFRD}(R, 0)} - 1 \quad (10)$$

where $\Sigma_*(R, 0)$ is the surface density profile of the stellar disc that we derive from the observed surface brightness profile.

Eq. 10 reveals that our parameter $\gamma(R)$ is ultimately a ratio between the stellar density and the current SFRD, given a certain formation time for the disc, which is of the order of the Hubble time and can be assumed roughly equal for all discs. A $\gamma(R)$ close to 1 means that the current SFR density extended to an Hubble time produces as many stars as observed at that location in the disc. Integrating $\gamma(R)$ over the disc and making use of eq. (8) we find an expression for the global γ as:

$$\gamma = \frac{2 M_*(0)}{(1 - \mathcal{R}) t_{\text{form}} \text{SFR}(0)} - 1 \quad (11)$$

where $M_*(0)$ and $\text{SFR}(0)$ are respectively the current stellar mass and star formation rate of the entire disc.

Clearly from eq. (11), one can also describe γ as proportional to the ratio between the average past SFR and the current SFR. This latter is the inverse of the so-called Scalo b -parameter (Scalo 1986) to which γ is closely related (see Section 3.2). We also note that any modification of eq. (7) with power law terms of $\frac{t}{t_{\text{form}}}$ would produce the same dependencies for γ as eq. (10). We discuss these points further in Section 4.2.

2.2 The star formation law

The main ingredient of our model is the relation between the rate of star formation and the gas density. The empirical star formation law is broadly accepted to be a power-law relation between the “cold” gas density and the star formation rate density (Schmidt 1959; Kennicutt 1998b). This relation has been tested on global (i.e. averaging gas and star formation on the whole disc) and local scales (Kennicutt et al. 2007) considering the molecular gas or the sum of atomic and molecular gas. Remarkably, it appears to hold across various orders of magnitudes, from quiescent discs to star-busting galaxies (Kennicutt 1998a; Krumholz et al. 2011). The dependence on gas metallicity is difficult to investigate due to the related dependency of the X_{CO} factor (Boissier

¹ Note that $\gamma(R) < 0$ would imply a lower formation time at that radius; this occurrence does not arise with our choice of parameters.

et al. 2003). However, the compilation of azimuthal averages of SFRD and Σ_{gas} presented by Leroy et al. (2008) for the THINGS sample, which includes galaxies with very different masses and presumably different metallicities, seems to show that the effect is limited (see Wyder et al. 2009, and Section 4.4). Thus, in the following we assume the following star formation law:

$$\text{SFRD} = A \Sigma_{\text{gas}}^N \quad (12)$$

with $N = 1.4$ and $A = 1.6 \times 10^{-4}$ if Σ_{gas} is measured in $M_{\odot} \text{pc}^{-2}$ and SFRD in $M_{\odot} \text{yr}^{-1} \text{kpc}^{-2}$ (Kennicutt 1998b). Note that the above value of A takes into account the correction for the presence of Helium (a factor 1.36 in mass), not applied in Kennicutt (1998b).

Deviations from the above relation are observed at column densities lower than $\Sigma_{\text{gas, th}} \simeq 10 M_{\odot} \text{pc}^{-2}$, referred to as the density threshold. Below these densities the law steepens and the scatter increases making it more difficult to describe (Schaye 2004; Bigiel et al. 2008). In the context of this paper, it may have an effect in the outer parts of the discs (see Sections 3.1 and 4.4).

Krumholz et al. (2012) have recently pointed out that the star formation law expressed in terms of volume density is more general than the one expressed in terms of surface density. This is very relevant to understand the physical origin of the law and to perform numerical simulations. However, for our investigation a surface-density law is far more practical. Clearly, the choices are equivalent if in the region of interest, i.e. within the star forming disc, the scale-height of the gaseous disc does not change much as a function of radius. The validity of this condition (within a factor 2) is well established in our Galaxy, as the disc appears to be flaring significantly only beyond $R \simeq 16 \text{ kpc}$ (Kalberla & Dedes 2008).

2.3 Inferring the gas accretion rate

The above assumptions on the SFH and the star formation law allow us to infer the local gas accretion rate using eq. (5). If the star formation law is described by eq. (12), the accretion rate density can be written as:

$$\begin{aligned} \dot{\Sigma}_{\text{ext}}(R, t) &= (1 - \mathcal{R}) \text{SFRD}(R, 0) f(R, t) \\ &\quad - \frac{\text{SFRD}^{1/N}(R, 0)}{N A^{1/N} t_{\text{form}}} f(R, t)^{\frac{1-N}{N}} \frac{\partial f(R, t)}{\partial t} \end{aligned} \quad (13)$$

where $\text{SFRD}(R, 0)$ is the current total gas density, A and N are the parameters of the star formation law and f is the functional form of the star formation history. The RHS of eq. (13) can also be expressed in terms of $\Sigma_{\text{gas}}(R, 0)$ (using the K-S law) instead of $\text{SFRD}(R, 0)$. This equation is general and it could be used if the *exact* shape of the SFH(R) were known. If f is given by eq. (7), the gas accretion rate density becomes:

$$\begin{aligned} \dot{\Sigma}_{\text{ext}}(R, t) &= (1 - \mathcal{R}) \text{SFRD}(R, 0) \left[1 + (\gamma(R) - 1) \frac{t}{t_{\text{form}}} \right] \\ &\quad - \frac{\text{SFRD}^{1/N}(R, 0)}{N A^{1/N} t_{\text{form}}} (\gamma(R) - 1) \left[1 + (\gamma(R) - 1) \frac{t}{t_{\text{form}}} \right]^{\frac{1-N}{N}} \end{aligned} \quad (14)$$

or, equivalently in terms of the gas density:

$$\begin{aligned} \dot{\Sigma}_{\text{ext}}(R, t) &= A(1 - \mathcal{R}) \Sigma_{\text{gas}}^N(R, 0) \left[1 + (\gamma(R) - 1) \frac{t}{t_{\text{form}}} \right] \\ &\quad - \frac{\Sigma_{\text{gas}}(R, 0)}{N t_{\text{form}}} (\gamma(R) - 1) \left[1 + (\gamma(R) - 1) \frac{t}{t_{\text{form}}} \right]^{\frac{1-N}{N}} \end{aligned} \quad (15)$$

The above equations give the rate at which fresh gas must be added to the disc at a certain radius and as a function of time to produce the star formation density given by $\text{SFRD}(R, t)$. As shown above, the shape of the SFH is regulated by the value of $\gamma(R)$. For $\gamma(R) = 1$, SFR and accretion are constant in time. More in general, when γ is close to 1 the second term on the RHS of eq. (14) is small leading to $\dot{\Sigma}_{\text{ext}}(R, t) \simeq (1 - \mathcal{R}) \text{SFRD}(R, t)$. Therefore the gas needed is directly proportional to the gas consumed by the star formation and this proportionality is simply $(1 - \mathcal{R})$. For $\gamma(R) > 1$ the second term in eqs. (14) and (15) becomes gradually more negative and less accretion is needed. High values of $\gamma(R)$ may result in a negative $\dot{\Sigma}_{\text{ext}}(R, t)$, hence at that time and radius, the amount of gas available in the disc exceeds what is needed by star formation. This would be the signature of an outflow of gas.

We define the global accretion rate $\dot{M}_{\text{ext}}(t)$ as the gas mass accreted per unit time over the whole galactic disc, obtained integrating eqs. (14) or (15) over the disc out to our maximum radius R_{m} . It is evident that the global accretion rate will have dependencies similar to those of the local one and the above considerations apply. In particular, for galaxies with γ of order unity, the global infall rate closely follows the SFR at every time $\dot{M}_{\text{ext}}(t) \simeq (1 - \mathcal{R}) \text{SFR}(t)$.

It is worth noting that $\dot{\Sigma}_{\text{ext}}(R, t)$ represents the gas surface density that has to be added to (or removed from) the disc per unit time to produce the reconstructed $\text{SFRD}(R, t)$. If we are considering a single annulus, $\dot{\Sigma}_{\text{ext}}(R, t)$ refers generically to the external environment including the adjacent annuli. Therefore, $\dot{\Sigma}_{\text{ext}}(R, t)$ coincides with the accretion (infall) rate at that radius only if there are no radial flows in the gaseous disc. This is because, with this method we do not trace the location of the gas infall but rather the radius at which such gas turns into stars. We discuss this issue a bit further later on. On the other hand, $\dot{M}_{\text{ext}}(t)$ represents the total mass needed to be accreted by the galaxy disc from outside, at the time t , to sustain the SFR at the reconstructed rate. Note however that also in this case the definition of *outside* the disc is merely *beyond* the maximum radius R_{m} assumed for the disc, which we took to be 5 times the scale-length of the stellar disc.

3 RESULTS

In this Section we apply the method described above to real galaxy discs. We impose the following *boundary conditions*: i) the current stellar density profile $\Sigma_{*}(R, 0)$, ii) the current SFR density profile $\text{SFRD}(R, 0)$. The latter could be in principle derived from the current gas density profile using the star formation law (Section 2.2). However here we restrict our analysis to cases where the current SFRD is known from independent estimates. We first consider the Milky Way and then a sample of spiral galaxies with known SFRD profiles.

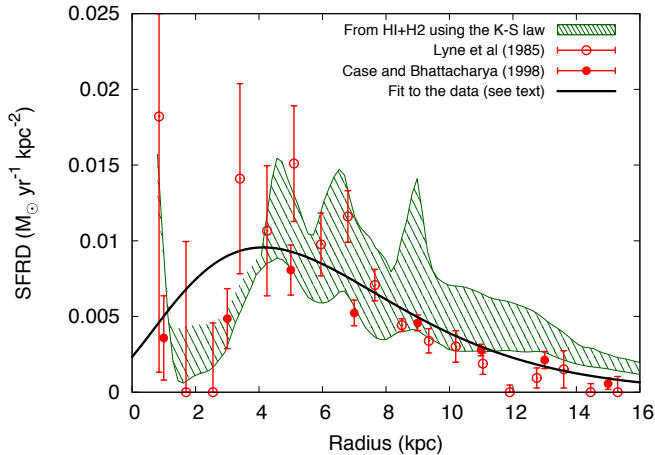


Figure 2. Current star formation rate density of the Milky Way disc estimated using pulsars (open squares), and supernova remnants (filled squares). These data, originally normalized to the Solar neighbourhood value, have been fitted with a function described in the text (solid line) and rescaled so that the integral over the disc gives $\text{SFR}(0) = 3 M_{\odot} \text{yr}^{-1}$. The shaded region shows the $\text{SFRD}(R, 0)$ one would get from the total (neutral + molecular) gas density using the K-S law. The lower and upper boundaries are due to the different determinations of the HI surface densities from Binney & Merrifield (1998) and Kalberla & Dedes (2008) respectively.

3.1 Application to the Milky Way disc

We assume that the stellar disc of the Milky Way is exponential with a scale length $h_R = 3.2 \text{ kpc}$ (Binney & Tremaine 2008) and a maximum extension of $R_m = 5 h_R$. The normalization of this profile is chosen so that the total stellar mass of the disc is $4 \times 10^{10} M_{\odot}$ (Dehnen & Binney 1998). The present distribution of the star formation rate density with respect to the Solar neighborhood, $\text{SFRD}(R, 0)/\text{SFRD}(R_{\odot}, 0)$, has been estimated using several methods. In Fig. 2 we show the estimates coming from the distribution of pulsars (open squares, Lyne et al. 1985) and supernova remnants (filled squares, Case & Bhattacharya 1998). We fit these points with a function (solid line in Fig. 2) of the form:

$$\text{SFRD}(R, 0) = \text{SFRD}(0, 0) \left(1 + \frac{R}{R_*}\right)^{\alpha} e^{-\frac{R}{R_*}}, \quad (16)$$

where $\alpha = 3.10$ is an exponent defining the tapering towards the centre and $R_* = 1.96 \text{ kpc}$ is a scale radius such that the peak of the distribution is located at $R = R_*(\alpha - 1)$. The central SFR density $\text{SFRD}(0, 0) = 2.3 \times 10^{-3} M_{\odot} \text{yr}^{-1} \text{kpc}^{-2}$ is normalized in order to have a global current star formation rate of the Milky Way $\text{SFR}(0) = 3 M_{\odot} \text{yr}^{-1}$ (see Table 1 in Diehl et al. 2006). The same normalization is then applied to the data points. The shaded region in Fig. 2 shows, as a consistency check, the SFRD inferred from the current total gas density using the K-S law. The upper and lower boundaries refer to two different determinations of the neutral gas density by Binney & Merrifield (1998) and Kalberla & Dedes (2008). The latter is not determined for $R < 4 \text{ kpc}$. The molecular gas density is taken from Nakanishi & Sofue (2006). On the whole the agreement between the direct determinations of SFRD and that inferred by the K-S law

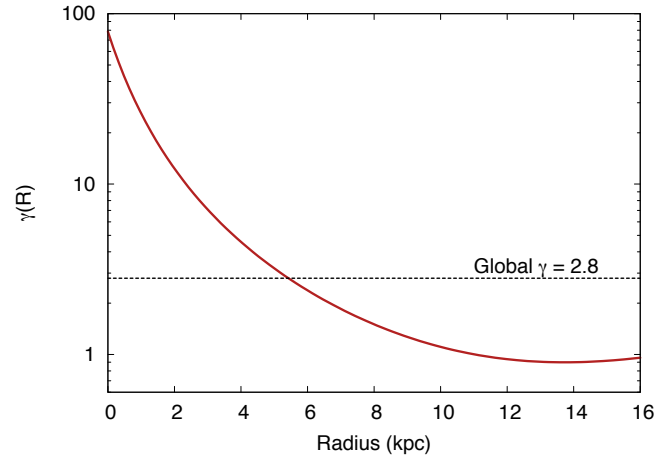


Figure 3. Steepness of the SFH as a function of radius for the Milky Way disc, parametrised by $\gamma(R)$ (see Section 2.1). The horizontal line shows the global value obtained for the whole disc.

is very good. In the outer parts the K-S predicts a larger SFR than observed, likely due to the low densities and the steepening of the law. We quantify this effect in Section 4.4. Some recent determinations of the current SFR of the Milky tend to give values around $1 - 2 M_{\odot} \text{yr}^{-1}$ (see e.g. Murray & Rahman 2010). However, Fig. 2 shows that only a $\text{SFR}(0) \simeq 3 M_{\odot} \text{yr}^{-1}$ is self-consistent with the derivation of the $\text{SFRD}(R, 0)$ from the gas surface density by inverting the K-S law, so we prefer to adopt this value throughout the paper. In the following we further fix the age of the stellar disc $t_{\text{form}} = 10 \text{ Gyr}$ or, equivalently, $z_{\text{form}} = 1.8$.² Note that taking a larger value for t_{form} , suggested for instance by the investigation of Aumer & Binney (2009) would strengthen our results.

We reconstruct the SFH of the Milky Way disc as described in Section 2.1. We find a steepness of $\gamma = 2.8$ for the whole disc. The behavior as a function of radius is shown in Fig. 3. The parameter $\gamma(R)$ appears to be a decreasing function of the radius R . Recalling that $\gamma(R)$ is the ratio between the initial and the current SFRDs, this trend shows, as expected, that star formation in the central regions must have been faster than in the outer disc, and it has spread from inside out (see also Naab & Ostriker 2006). Note that our approach is fully axi-symmetric and it does not account for the presence of a bar, thus our results for $R \lesssim 3 \text{ kpc}$ should be taken with some caution.

The SFR(t) of the Galaxy reconstructed using the linear temporal dependency of eq. (7) is shown in Fig. 4 (top panel) ($\gamma = 2.8$). We remind that the key parameters to obtain this curve are the current SFR and the current stellar mass of the disc (eq. 11). Changing these parameters and the formation time of the disc (t_{form}) would produce rather intuitive variations in the value of γ and the steepness of the SFH. Extreme values can be obtained by taking $\text{SFR}(0) = 2 M_{\odot} \text{yr}^{-1}$, $M_*(0) = 5 \times 10^{10} M_{\odot}$ and $t_{\text{form}} = 8 \text{ Gyr}$ on the one hand and $\text{SFR}(0) = 4 M_{\odot} \text{yr}^{-1}$,

² We assume a standard cosmology with $\Omega_b = 0.27$ and $\Omega_{\Lambda} = 0.73$.

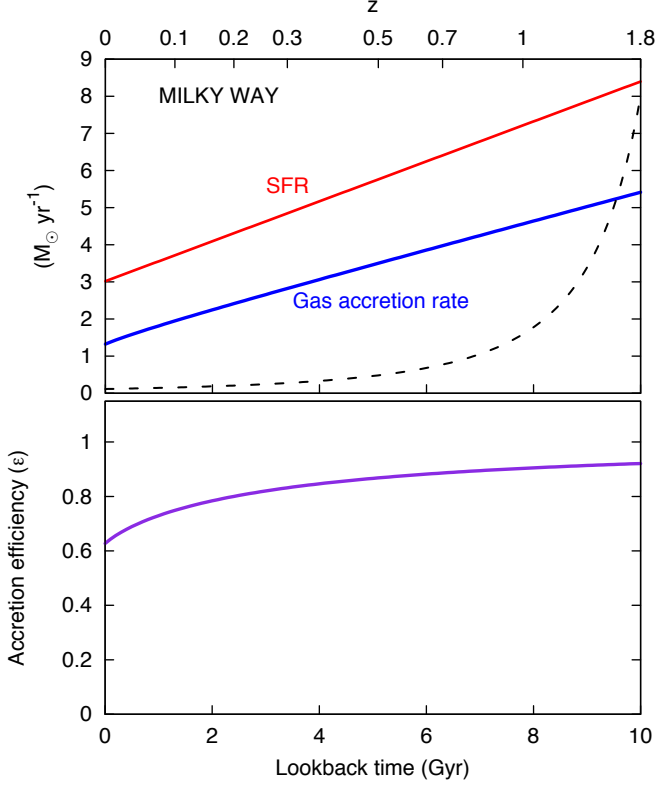


Figure 4. *Top panel:* SFR and global gas accretion rate, versus time and redshift for the disc of the Milky Way. The dashed line shows the evolution of a closed box. *Bottom panel:* Gas accretion efficiency as a function of time, $\varepsilon = 1$ corresponds to a complete replenishment and thus a constant SFR.

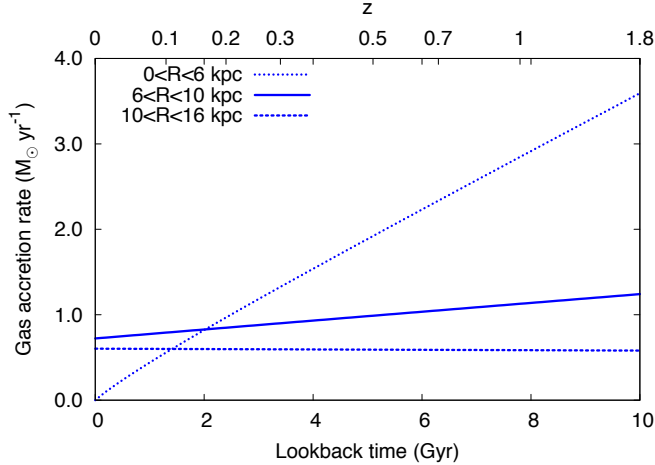


Figure 5. Gas accretion into the Milky Way’s disc integrated over three annuli centered at 3 kpc (short dashed line), 8 kpc (solid line) and at 13 kpc (long dashed line) versus time and redshift.

$M_*(0) = 3 \times 10^{10} M_{\odot}$ and $t_{\text{form}} = 12$ Gyr on the other, corresponding to $\gamma_{\text{max}} = 7.9$ and $\gamma_{\text{min}} = 0.8$ respectively.

Having derived $\gamma(R)$ we can proceed to estimate the gas infall rate at each radius and its global value by integrating over the whole disc surface using eq. 14. Fig. 4 shows the global gas accretion rate necessary to maintain

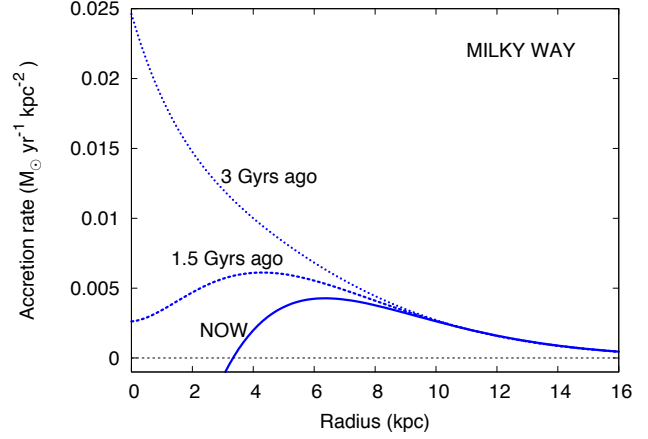


Figure 6. Gas accretion profile at three epochs: lookback time = 3 Gyr, 1.5 Gyr, and now. Note the very recent development of an inner depression and of a peak in the gas accretion distribution, now at about $R_{\text{peak}} \simeq 6 - 7$ kpc from the Galactic centre.

the star formation in the Milky Way disc. The accretion rate is positive at every redshift starting from $5.4 M_{\odot} \text{ yr}^{-1}$ at t_{form} and decreasing to $1.3 M_{\odot} \text{ yr}^{-1}$ at the current time. It follows very closely the shape of the SFR. These results are in agreement with earlier determinations based on chemical evolution models (e.g. Tinsley 1980; Tosi 1988a). In the same figure, we also plot the SFR that our Galaxy would have if it evolved like a closed system starting from the same initial conditions. A closed system is only able to produce $\simeq 8.4 \times 10^9 M_{\odot}$ of stars from $t = t_{\text{form}}$ to $t = 0$, virtually leaving no remnant gas mass at present. On the contrary, our model with gas infall predicts a present total gas mass of $7.1 \times 10^9 M_{\odot}$, comparable to what observed. The bottom panel of Fig. 4 shows the gas accretion efficiency defined as the ratio of the accretion rate over the net gas-consumption including feedback, $\varepsilon(t) = \dot{M}_{\text{ext}}(t)/(1 - \mathcal{R})\text{SFR}(t)$. For the whole disc of the Milky Way we obtain $\varepsilon_{\text{MW}}(t) \sim 0.6$ at $t = 0$. $\varepsilon_{\text{MW}}(t)$ has a mild dependence on time, reaching a value of about 0.9 at $z = 1$. This shows that the efficiency of gas accretion is rather high but not enough to keep the SFR constant ($\varepsilon = 1$). Thus, gas accretion does not feed the discs indefinitely, however it delays the running-out of fuel significantly beyond the (closed-box) gas-consumption timescale. The value of the current accretion rate and efficiencies are rather uncertain as they strongly depend on the assumed zero-points. For instance, leaving all the other parameters unchanged and taking $\text{SFR}(0) = 2 M_{\odot} \text{ yr}^{-1}$ would give a current accretion of only $0.14 M_{\odot} \text{ yr}^{-1}$. This large difference is totally localized to the current time, indeed the efficiency of accretion remains always above 0.5 from the disc formation to $z = 0.1$ plunging then to 0.1 at $z = 0$, see also the case of NGC 5055 in Section 3.2.

We now turn to the local infall rate $\dot{\Sigma}_{\text{ext}}(R, t)$. For visualization purposes, we split the galaxy in three representative zones: the central part (between 0 – 6 kpc), the solar circle (6 – 10 kpc) and the outer disc (10 – 16 kpc). For each region we calculate the local gas accretion rate integrating over the annulus surface and we plot the results in Fig. 5. We find three different regimes: i) in the central region the gas accretion declines very steeply, ii) in the solar circle the

gas accretion declines by a factor 1.7, iii) in the outer disc it increases slightly reaching its maximum at $z = 0$. The behaviour visible in Fig. 5 reflects the simple fact that the ratio between the stellar density and gas density decreases strongly with radius in the Galaxy. The same kind of trends are visible in the SFH reconstructed for the same annuli, given that as seen above, $\dot{\Sigma}_{\text{acc}}(R, t) \sim (1 - \mathcal{R})\text{SFRD}(R, t)$.

Fig. 6 shows the gas accretion profile as a function of R in the Milky Way's disc now and at two epochs in the recent past. The current profile is negative for $R < 3$ kpc, peaks at about $R = 6$ kpc and then falls further out. The negative value in the central regions shows that there the amount of gas is sufficient to sustain the star formation and the model would predict outflow (of about $0.2 M_{\odot} \text{yr}^{-1}$). This inner feature is of recent formation as 3 Gyrs ago the peak of accretion was right in the centre. So we conclude that the bulk of gas accretion is moving away from the inner disc. As a consequence star formation also moves out although with a delay with respect to the accretion. Note that the shape of the accretion profile at $t = 1.5$ Gyr is remarkably similar to the current $\text{SFRD}(R, 0)$ (see Fig. 2), hinting at a delay between accretion and star formation of a Gyr or so. Interestingly, this is of the order of the gas depletion timescale.

We stress again that with our approach we are able to trace the locations in the disc where the new gas begins to form stars. The infall itself could have happened somewhere else, realistically more further out and the infalling gas could have quiescently flown to inner radii before starting forming stars and becoming *detectable* by our method.

3.2 External galaxies

In this Section we extend the application of our method to a sample of external galaxies. We consider galaxies from the THINGS survey (Walter et al. 2008) for which radial profiles of gas density and SFRD are available (Leroy et al. 2008). As for the Milky Way, we assume a common return factor $\mathcal{R} = 0.3$, an age of the discs of $t_{\text{form}} = 10$ Gyr and the linear $f(t)$ described in Section 2.1. We derive the global values of γ both using eq. (11) and by integrating $\gamma(R)$ (eq. 10) over the disc. In the former case the values of stellar masses and SFRs were taken from Table 4 of Leroy et al. (2008), in the latter we used their SFR densities available online. The two methods led, in some cases, to significantly different values for γ . This is partially due to the different range of integration, Leroy et al. (2008) integrate out to $1.5 R_{25}$ while we integrate out to 5 scale-lengths (when the profiles extend this far, i.e. for roughly for half of the galaxies) for consistency with the Milky Way analysis.

Fig. 7 shows the derived values for the global γ as a function of the stellar mass (top) and Hubble type (bottom), the black star shows the Milky Way. The bars show the ranges allowed by the two methods described above. Note that for some galaxies also the stellar masses resulting from our integrations differ from those of Leroy et al. (2008). The values of γ inferred for these galaxies are all included between 0 and 11, with one outlier at $\gamma = 23$, NGC 2841, a massive Sb galaxy with rather low current SFR (shown only in the top plot). There is a clear trend with stellar mass and Hubble type, showing that big galaxies had much larger SFRs in the past. On the other hand, low values of γ , typical for

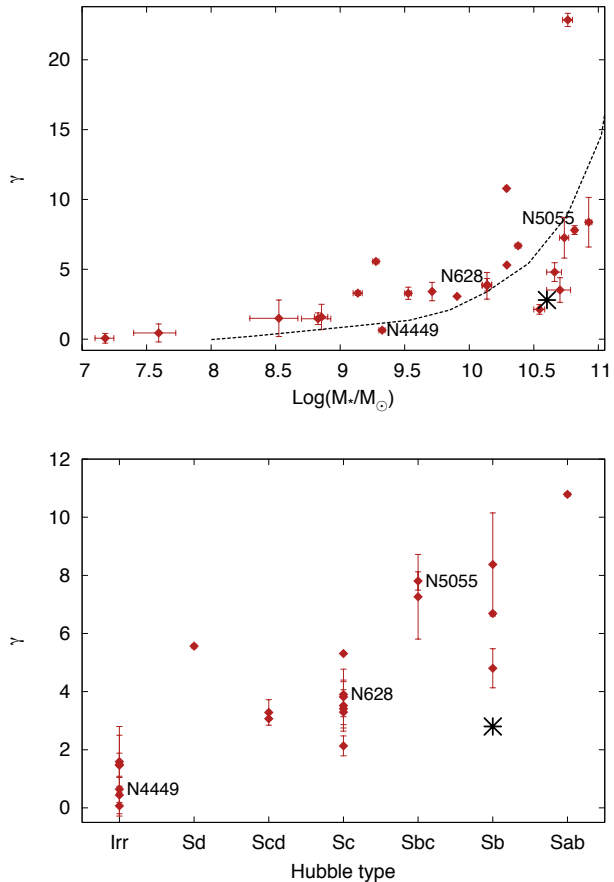


Figure 7. The (disc-integrated) parameter γ (steepness of the SFH) for the sample of 21 disc galaxies of Leroy et al. (2008) as a function of the stellar mass (*top panel*) and galaxy type (*bottom panel*). The star indicates the Milky Way. A common time of disc formation of 10 Gyr and the SFH-function $f(t)$ have been assumed for all galaxies. The error-bars show the interval allowed by two different methods of integration described in the text. The dashed curve in the top panel shows the value of γ derived from the Scalo b -parameter for the SLOAN survey (Brinchmann et al. 2004).

smaller galaxies betray a disc continuously forming through the acquisition of fresh gas.

As mentioned, we can relate our γ to the Scalo b -parameter. We use the recent determination of b versus stellar mass relation from the SDSS (Brinchmann et al. 2004) and convert it into γ . We plot this relation as a dashed curve in the top panel of Fig. 7. The two parametrisations agree remarkably well, considering that they are derived in completely different ways. Our values tend to be slightly above the curve for masses lower than 10.5 in the log and below for larger masses. This is likely due to the shape adopted for the SFH, see discussion in Section 4.2. Note that, in this respect, Fig. 7 is analogous to Fig. 3 in Kennicutt (1998a).

For the above disc galaxies we have performed the same analysis as for the Milky Way. We derived the radial profiles of $\gamma(R)$ and $\Sigma_{\text{ext}}(R, t)$ and integrated the latter to derive the global accretion rates. Fig. 8 shows the results for three galaxies representative of three classes of stellar masses and galaxy types (see labels in Fig. 7). In general, small late-type

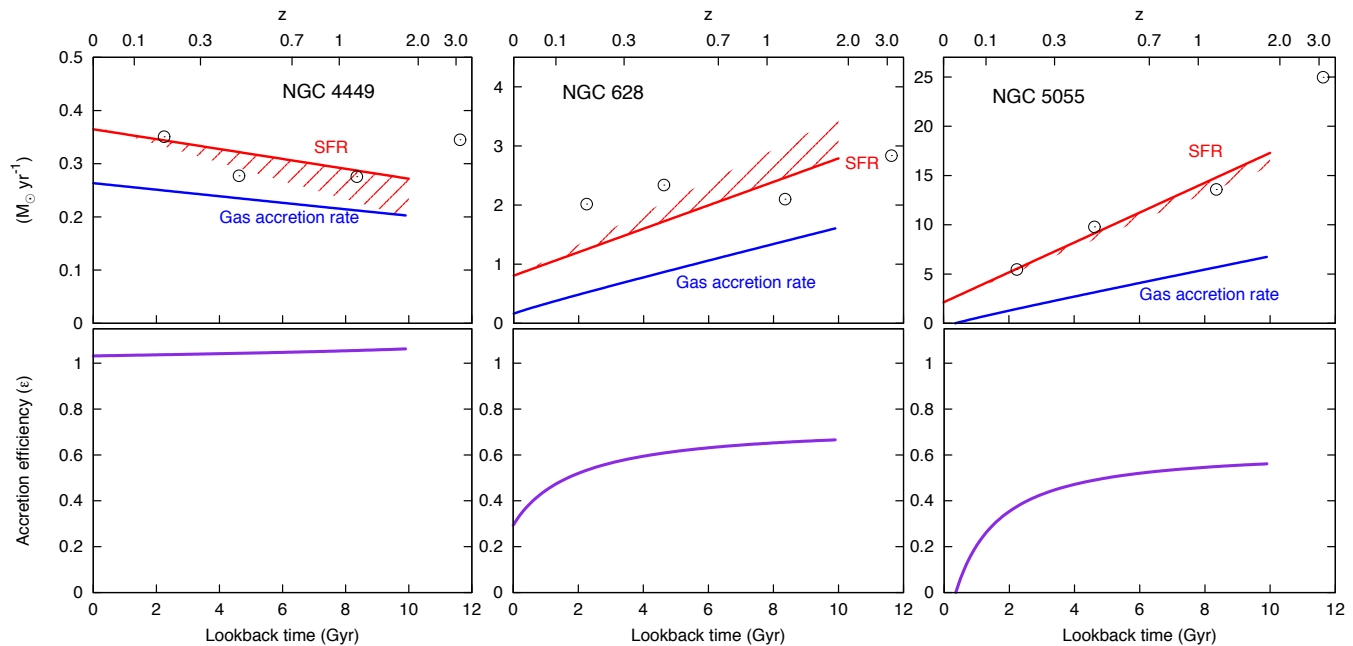


Figure 8. *Top panels:* SFRs and gas accretion rates as a function of time for three representative galaxies from the sample of Leroy et al. (2008). The shaded areas show the uncertainties in the determination of the global γ described in the text. The open dots are the average SFHs estimated by Panter et al. (2007) for galaxies of the same stellar masses. *Bottom panels:* Gas accretion efficiencies as a function of time, $\epsilon = 1$ corresponds to a complete replenishment and thus a constant SFR with time.

galaxies tend to have a flatter SFH and an efficiency of gas accretion close to 1, see the case of NGC 4449 (left panels). Galaxies of intermediate types have a shallower SFR and efficiency gradually decreasing with time. Finally, massive discs with low current star formation rates seem to have exhausted their capability of acquiring significant amount of gas from the environment. They now appear to be consuming their remnant gas before moving to the red sequence (e.g. Cappellari et al. 2011). In the same Fig. 8 we also compare our results with the average SFHs derived using the SLOAN survey by Panter et al. (2007), shown as open circles. Panter et al. divide their galaxies in bins of current stellar masses, those relevant here are $3 \times 10^{10} < M_* < 1 \times 10^{11}$, $1 \times 10^{10} < M_* < 3 \times 10^{10}$, $M_* < 1 \times 10^{10}$, respectively applicable for NGC 5055, NGC 628, and NGC 4449. The agreement between our SFRs and their average SFRs is very good, except for the galaxies in the intermediate mass class as our method tends to find steeper SFHs. Note however that this may also depend on the way the stellar masses are estimated. We used the estimate of Leroy et al. (2008) who simply multiply the 3.6- μm surface brightness by a constant mass-to-light ratio of 0.5.

In general, the analysis of these 21 THINGS galaxies gives results similar to those found for the Milky Way’s disc. Gas accretion proceeds almost parallel to the SFR and it remains significantly important throughout a large fraction of the lifetime of a typical disc galaxy. The efficiency of accretion seems to decrease fast for large galaxies, while small late-type discs remain quite efficient in collecting cold star-forming gas from the environment. The current ($z = 0$) values of gas infall that we derive are quite low for most galaxies in the sample and a few also have negative values showing that the available gas is more than sufficient for star formation to proceed. Thus, it would appear that

these disc galaxies do not need gas accretion to sustain their current star formation (see e.g. NGC 5055). This is potentially a very interesting result but unfortunately, as shown for the Milky Way, these values are very uncertain because they come from an extrapolation. Moreover, they depend on parameters like the stellar masses that have intrinsic uncertainties and other parameters that are simply assumed (see eq. 14). For instance if one increases the formation time of the disc or decrease the return factor the value of the current accretion rate may increase substantially. What remains indisputable is the fundamental relation between star formation and accretion and the fact that the latter *must* be a major player in the evolution of galaxies from their formation to the present. There is no way a disc galaxy could become as we see it today without substantial gas infall at $z < 1$.

4 DISCUSSION

In the previous Sections we have shown how a simple comparison between the stellar density in galactic discs and their current SFRD (or gas density) implies the need for a large amount of gas infall during their lifetimes. This need is rooted in the existence of the Kennicutt-Schmidt law and in the assumption that this does not significantly evolve with time. Under this assumption we were able to derive the accretion rates as a function of galactocentric radius and time for a number of disc galaxies including the Milky Way. Here we discuss the limitations of our approach and the implications of our results.

4.1 Delayed stellar feedback

Treating stellar feedback with the I.R.A. saves computing time and it allows us to write simple analytic expressions for the equations of the model, however the delayed return from stars with mass $M < 8 M_\odot$ may be an important effect that needs to be quantified. We added this ingredient using the approximation that a star with mass M returns a fraction $\eta(M)$ of its mass to the interstellar medium at a time $t_{\text{MS}}(M)$ (see Kennicutt et al. 1994). The stellar lifetime (t_{MS}) are taken from Maeder & Meynet (1989):

$$t_{\text{MS}}(M) = 12 \left(\frac{M}{M_\odot} \right)^{-2.78} \text{ Gyr} \quad M \leq 10 M_\odot$$

$$0.11 \left(\frac{M}{M_\odot} \right)^{-0.75} \text{ Gyr} \quad M > 10 M_\odot \quad (17)$$

given that $t_{\text{MS}}(1 M_\odot) > 10$ Gyr stars below $\sim 1 M_\odot$ do not contribute to the feedback. The difference between the I.R.A. and the delayed return is that the term $\dot{\Sigma}_{\text{fb}}$ in eqs. (1) and (2) becomes:

$$\dot{\Sigma}_{\text{fb}} = \int_{M_{\text{min}}(t_{\text{form}}-t)}^{100} \text{SFRD}(t + t_{\text{MS}}(M)) \eta(M) \phi(M) dM \quad (18)$$

where $\phi(M)$ is the IMF. The integration is performed from $M_{\text{min}}(t_{\text{form}} - t)$, which is the mass of a star with a MS time equal to the age of the disc at that time (Prantzos 2008); note that with t we indicate, as usual, lookback time. In order to calculate $\gamma(R)$ with delayed feedback, we have numerically integrated eq. (1) from the present to t_{form} using eqs. (6) and (7) for $\text{SFRD}(R, t)$. At each radius R , the integration has been repeated iteratively until we matched the observed stellar surface brightness $\Sigma_*(R, 0)$. Then the global γ was calculated using eq. (11). Finally the accretion rate as a function of radius and time was derived using eq. (14).

Fig. 9 shows the comparison between the global SFR and accretion rate for the Milky Way with I.R.A. and with delayed stellar feedback. The values of current SFR and stellar mass are kept fixed in both cases. As expected the global gamma with delayed feedback is lower, $\gamma_{\text{DF}} = 2.7$ (2.6 for a Chabrier IMF), than that with I.R.A. This is because if the mass return to the ISM is delayed then fewer stars need to form in order to have the same stellar mass at the present time. The gas accretion is higher at the beginning due to the fact that less gas is available from stellar recycling and becomes slightly lower later on when feedback from low mass stars becomes important. The bottom panel of Fig. 9 shows the accretion efficiency calculated with and without delayed feedback. Accretion with delayed feedback tends to have a slightly larger efficiency. However the shape of the two curves is exactly the same and the difference in the normalization is minor. In conclusion, including delayed feedback in our calculations makes little difference and it goes in the direction of increasing the efficiency of gas accretion.

4.2 Parametrisation of the SFH

The reconstruction of the star formation rate density as a function of time requires the parametrisation of the SFH. In Section 2.1 we have chosen a simple first order polynomial. We also point out that a more general power-law would give similar dependencies for $\gamma(R)$. Here we consider three dif-

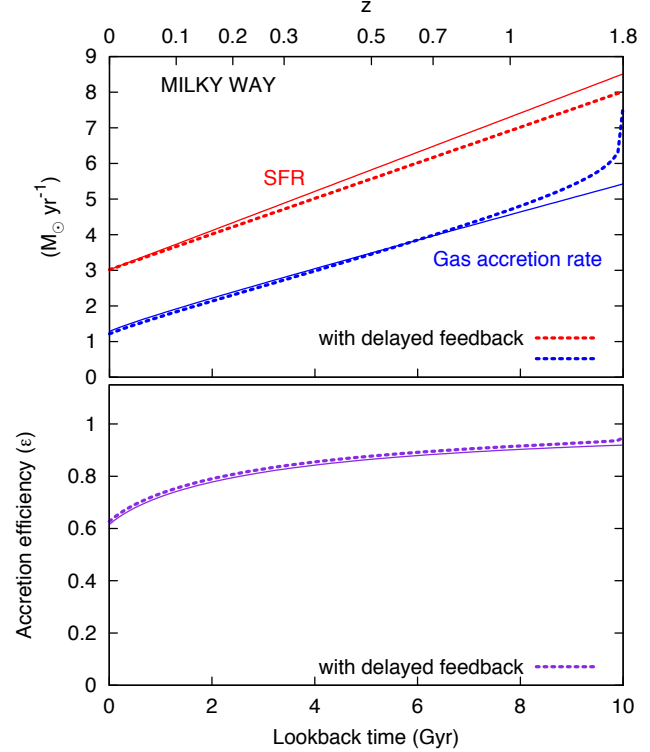


Figure 9. *Top panel:* SFR and global gas accretion rate, versus time and redshift for the disc of the Milky Way with instantaneous recycling approximation (thin solid lines) and delayed feedback (thick dashed lines). *Bottom panel:* Gas accretion efficiency as a function of time with instantaneous recycling approximation (thin solid line) and delayed feedback (thick dashed line).

ferent parametrisations and show that our results do not change significantly. We take the following functional forms: i) a piecewise-linear function of time $f_2(t)$ that linearly increases to a maximum SFR at $t = t_c$ and remains constant at higher lookback times; ii) a triangular function of time $f_3(t)$ that linearly increases to a maximum SFR at $t = t_c$ and then decreases to $\text{SFR}(0)$ at $t = t_{\text{form}}$; iii) an exponential function of this form: $f_4(t) = e^{t/\tau}$ where τ is the exponential e -folding time of the SFR. With these choices we encompass both monotonic and non-monotonic functions. In ii) γ is defined as the ratio between $\text{SFR}(t_c)/\text{SFR}(0)$.

In Table 1, we show the values of the global γ , and the present accretion rate $\dot{M}_{\text{ext}}(0)$ and accretion efficiency $\epsilon(0)$ obtained with the four types of $f(t)$ for the Milky Way. We took $t_c = 7.7$ Gyr ($z_c = 1$). For the exponential function, often used for early type galaxies (e.g. Bell et al. 2003), we found a rather long scale-time of $\tau = 8.5$ Gyr and a shape of the SFH very similar to that obtained with $f_1(t)$. Even though these three functions depict very different trends for the SFH, the disc-integrated γ varies only by $\sim 17\%$ and the values of the present accretion rate and $\epsilon(0)$ change by no more than 13 %. Note that the inverse of the Scalo b -parameter would correspond to a piece-wise linear functional form $f_2(t)$ for $t_c \rightarrow 0$. All the above values are obtained using the I.R.A. Using the delayed return with different shapes of the SFH can produce different effects. For instance an exponential SFH of the type $f_4(t)$ maximizes the gas con-

| $f(t)$ | γ | $\dot{M}_{\text{ext}}(0)$ | $\varepsilon(0)$ |
|-----------------------|----------|---------------------------|------------------|
| linear (1) | 2.8 | 1.31 | 0.62 |
| piece-wise linear (2) | 2.5 | 1.27 | 0.61 |
| triangular (3) | 2.4 | 1.21 | 0.58 |
| exponential (4) | 3.2 | 1.49 | 0.71 |

Table 1. The effect of using different parametrisations for the SFH described in the text. γ is always defined as the ratio between the initial over the current SFR except for the triangular function where it is the ratio between the SFR at $z_c = 1$ over the current value.

sumption timescales, which can increase up to a factor 2 – 3 at the earliest times (see Kennicutt et al. 1994).

4.3 Effect of stellar migration

In the above we have assumed that radial motions of stars in the disc are not significant, here we relax this assumption and estimate the effect of a global migration (e.g. Roškar et al. 2008; Minchev et al. 2011). For simplicity we take an exponential stellar profile with central surface brightness $\Sigma_*(0)$, a scale length h_R , and a maximum extent at radius $R_m = 5 h_R$. The stellar mass of the disc is:

$$M(\Sigma_*(0), h_R) = 2\pi\Sigma_*(0)h_R^2 \left[1 - e^{-\frac{R_m}{h_R}} \left(1 + \frac{R_m}{h_R} \right) \right] \quad (19)$$

Consider now a radial motion with a constant velocity v at R_m that lasts a time t directed inward or outward. Since the initial stellar profile is truncated beyond R_m , all stars at this radius will move to the new position $R_m + vt$, which represents a new maximum radius and is greater or smaller than R_m depending on the sign of v . This condition translates to the following relation involving the new (i.e. after migration) stellar profile Σ'_* :

$$\Sigma'_*(R_m + vt) = \Sigma_*(R_m) \quad (20)$$

that, together with the assumption that the profile remains exponential and that the mass is conserved:

$$M'(\Sigma'_*(0), h'_R) = M(\Sigma_*(0), h_R), \quad (21)$$

allows us to estimate $\Sigma'_*(0)$ and h'_R , the new central surface brightness and scale length.

In Table 2 we report the variation of the exponential profile of the Milky Way ($\Sigma_*(0) = 648.2 M_\odot \text{pc}^{-2}$ and $h_R = 3.2$ kpc) in the presence of coherent radial motions. When the flow of stars is directed inward, obviously the normalization of the stellar profile increases and the scale length decreases. Eq. (10) tells us that $\gamma(R) + 1 \propto \Sigma_*(R)$. Therefore, the profile of $\gamma(R)$ will change to $\gamma'(R)$ according to this relation:

$$\gamma'(R) = \frac{\Sigma'_*(R)}{\Sigma_*(R)}(\gamma(R) + 1) - 1 \quad (22)$$

For radii R where $\Sigma'_*(R)/\Sigma_*(R) > 1$, eq. (22) predicts an increase in the parameter $\gamma(R)$ and vice versa for $\Sigma'_*(R)/\Sigma_*(R) < 1$. This can be explained considering that a radial motion that brings more stars at a certain radius (i.e. $\Sigma'_*(R)/\Sigma_*(R) > 1$) makes the latter as it had been *more star-forming*. Despite the changes in $\gamma(R)$ it is remarkable that the new global γ changes very little, see the rightmost

| $vt[\text{kpc}]$ | Σ'_* | h'_R | $(\gamma'/\gamma)_{\text{MW}}$ |
|------------------|-------------|--------|--------------------------------|
| -3 | 1226.96 | 2.31 | 1.25 |
| -2 | 980.63 | 2.59 | 1.08 |
| -1 | 792.97 | 2.88 | 1.02 |
| 0 | 648.22 | 3.2 | 1.00 |
| 1 | 534.77 | 3.54 | 1.04 |
| 2 | 444.79 | 3.89 | 1.12 |
| 3 | 372.61 | 4.27 | 1.21 |

Table 2. The effect of radial migration of stars on an exponential stellar profile and on the disc-integrated γ for our Galaxy

column of Table 2, showing that our global results are only slightly affected by radial migration.

Sellwood & Binney (2002) showed that the dominant effect of spiral waves in galaxy discs is to churn the stars in a manner that preserves the overall angular momentum distribution. Stars move both inwards and outwards without any significant radial spreading of the disc or increase in non-circular motions. In their Fig. 13 they plotted the final distribution of home radii for six different radial bins for our Galaxy. The distributions are roughly Gaussian for every radial bins, with the largest dispersion $\sigma \simeq 3$ kpc at about R_\odot . So as to give an upper limit on this effect we infer the new stellar profile $\Sigma_*(R)'$ as the average of that modified by inward radial motion with parameter $vt = -3$ kpc and that of an outward motion with parameter $vt = 3$ kpc. We found that the changes in $\gamma(R)$ are significant for some radii but there is basically no effect on the global value of γ . We conclude that both migration and random redistribution of stars over the disc do not affect our global results.

4.4 Comparison to other studies

It is a matter of debate whether galaxies had their reservoir of gas in place from the beginning or they have been harvesting the gas they needed throughout their lives. We find that the second must be the case for all late type galaxies. A concentration of gas as large as the current disc stellar masses would imply an extremely high SFR at earlier times, a sudden formation of most of the stars and a steeply declining star formation at later times. This is how a red sequence galaxy forms and evolves. Galaxies like the Milky Way or spirals of later types clearly did not have this kind of star formation history. The evidence comes from the reconstruction of the star formation histories from the color magnitude diagrams (e.g. Harris & Zaritsky 2009), from chemical evolution models (e.g. Chiappini et al. 2001), and from cosmology (e.g. Hopkins et al. 2008). Our study further supports this point making use of the Kennicutt-Schmidt law.

A possible way out would be to invoke a variation of the K-S law with redshift or with metallicity as proposed by e.g. Krumholz & Dekel (2011). However, to reconcile the observations with negligible accretion at $z < 1$ the variations in the K-S law should be very large. If one required the initial gas mass of the Milky Way disc to be as large as the stellar mass today, the K-S law would imply an initial SFR of $\sim 50 M_\odot \text{yr}^{-1}$. At that rate, the stellar disc would form in a Gyr and the subsequent evolution would be passive (similar shape to the closed-box shown in Fig. 5). Therefore to keep the current SFR at the observed value the transformation

of gas into stars should have been an order of magnitude less efficient than the K-S law would predict. Moreover, this efficiency should have evolved with the galaxy itself in order to keep the star formation roughly constant in time. This is in contradiction with the fact that today galaxies with very different masses and thus different disc metallicities roughly follow the same K-S law (Leroy et al. 2008). Thus, it seems unlikely that any realistic evolution of the K-S law can account for the evolution of discs without conspicuous gas accretion at $z < 1$.

Despite the lack of metallicity information in our analysis, we have tried to quantify the above effect by assuming a different star formation law for low density environments. To this aim, we broke the star formation law into two parts: we assumed that the standard K-S is valid only down to a break surface density of $10 M_{\odot} \text{pc}^{-2}$ in hydrogen, below which the law takes a different form. We took this form from the work of Roychowdhury et al. (2009) who studied a compilation of extremely faint (and presumably metal poor) dwarf galaxies and found that a normalization of $A = 1.0 \times 10^{-5}$ and a slope of $N = 2.47$ are suitable for these low density environments. This parametrisation makes star formation less efficient at low gas densities. We repeated all the above calculations and found that the general result is, as expected, that more accretion is required, because star formation needs more gas to occur at the same rate. However, the differences are not big. For instance the amount of gas in the Milky-Way disc at all times increases by a factor in the range 9 – 18% and the amount of accretion today only by 5%. For the other galaxies the differences can, in some cases, go up to a factor ~ 2 . The reason for this is that the second term on the r.h.s. of eq. (14) does not change by more than a factor 2.3 below the break surface density.

Another important result of our investigation is that gas accretion moves in time from the central to the outer parts of the discs. In other words, the inner parts dominate the accretion at earlier times, whilst the outer parts dominate at later times, see Fig. 5. This inside-out evolution is also responsible for the production of metallicity gradients (see e.g. Matteucci et al. 1999; Boissier & Prantzos 1999). The progressive shift of accretion may be related to the angular momentum of the infalling material and it would be interesting to check it against the results of ab-initio hydrodynamical simulations (e.g. Piontek & Steinmetz 2011, and references therein).

Our model also predicts the distributions of stars and gas in the disc at all times. We found that the stellar disc of the Milky Way remains roughly exponential, at least in the inner parts, with a scale-length slightly increasing with time from 2.7 to 3.2 kpc. The gaseous disc, initially exponential, develops an inner depression with time, as stars are formed in the central region and the accretion becomes more and more efficient in the outer parts. Fig. 10 shows the evolution of the stellar and gaseous masses in the Milky Way disc. The cumulative stellar mass increases slowly with time. Roughly 2/3 of the stars formed at $z < 1$ as a consequence of gas accretion towards the inner disc. On the other hand, the gas mass remained almost constant and always rather low. Interestingly, the ratio between our initial and current gas mass for the Milky Way is the same as that obtained by comparing the HI mass in galaxies at $z = 0$ with that of Damped Ly α systems (e.g. Zwaan et al. 2005; Lah et al.

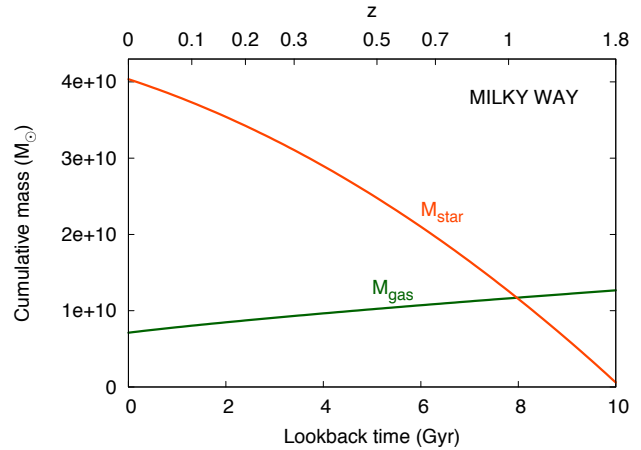


Figure 10. Gaseous and stellar mass as a function of the lookback time in the disc of the Milky Way.

2007). We stress again that the gas total mass in Fig. 10 is calculated within $R_m = 5 h_R$, more gas may lay at larger radii and flow inwards with time.

In a recent paper Naab & Ostriker (2006) built a model for the evolution of the Milky Way that has aspects in common to our investigation. They consider the growth of a disc that goes through an initial merger phase that lasts about 2 Gyr and then follows a quiescent evolution. This second phase is analogous to the phase we are considering in this paper. Naab & Ostriker (2006) assume the variation of the scalelength of the disc with time as the inverse of the Hubble parameter, so by a factor about 3 in the last 10 Gyr. This assumption together with the K-S law, used to derive the SFR, determine the amount of gas accretion onto the disc. In contrast to this approach, we derive the SFRD(R, t) from the normalization at redshift zero and use the K-S law to derive the amount of gas available at any time and the amount of gas needed (gas accretion) to reproduced that SFRD(R, t). Then from this we obtain the evolution of the stellar and gaseous discs.

From the above it is clear that the methods used in the present paper and in Naab & Ostriker (2006) are rather complementary and it is remarkable that we attain a very similar evolutionary picture for the Galaxy disc. The main difference is the evolution of the stellar-disc scalelength, which evolves qualitatively in the same way but quantitatively much less in our treatment, i.e. our disc has initially $h_R \simeq 2.7$ kpc as opposed to $h_R \sim 1$ kpc in their model (see their figure 1). The SFRs in the Solar neighbourhood are slightly different but both comparable with the determination of Rocha-Pinto et al. (2000). Finally, they also find that the accretion rate closely follows the SFR at every time and at present is about $2 M_{\odot} \text{yr}^{-1}$, slightly higher than ours. Our analysis also shows similarities to the work of Boissier & Prantzos (1999). These authors choose a different form of the star formation law and derive chemical and spectrophotometric properties of the Milky-Way disc. In their case, the accretion-rate is fixed and assumed to take an exponential law. Globally, all these descriptions give a consistent picture of the evolution of a galactic disc, reinforcing the validity of the different parametrizations.

4.5 What type of accretion?

Our treatment does not include metallicity information but it is clear that the infalling gas is bound to be at low metallicity. The need for metal-deficient accretion has been shown and confirmed throughout the last decades starting from pioneering works such as Tinsley & Larson (1978) and Tinsley (1980). More recently it has become clear that one needs two epochs of gas infall: one at the early epochs and one slower and still ongoing, which is the one we are describing here (Chiappini et al. 1997). The metallicity of this gas should be fairly low, of order $0.1 Z_{\odot}$ or less (e.g. Tosi 1988b). The origin of this accretion is still matter of debate and it is beyond the scope of this paper. As mentioned, several numerical investigations show that cooling of the hot corona may provide a reasonable amount of gas accretion onto the Milky-Way disc, although at a relative low rate (Peek et al. 2008; Kaufmann et al. 2009). These simulations roughly reproduce also the kinematics of this gas (Kaufmann et al. 2006) and the radial distribution of the accretion (Peek 2009). However, the whole mechanism of direct cooling via thermal instability has been recently challenged both by analytical analyses (Binney et al. 2009; Nipoti 2010) and by recent grid-based simulations (Joung et al. 2011) and the matter is still not settled.

Our accretion is smooth but this is obviously an artifact of our assumptions. In principle the main contribution to gas infall could be minor mergers with gas rich satellites, which would give presumably a more bursty SFH. In this sense, our analysis is still applicable if one averages all quantities over a time larger than the typical starburst timescale. Current HI observations seem to show that the amount of gas that can be realistically brought into large galaxies by gaseous satellites in the local Universe is rather low (Sancisi et al. 2008). However, these estimates are still uncertain and only future HI surveys will allow us to determine the accretion from mergers with the required accuracy. A recent analysis of the contribution of satellites to the gas accretion in the Milky Way shows that they would also not reproduce the distribution of SFR observed today (Peek 2009).

Finally, we found that accretion and star formation proceed together. This is clear from eq. 13 and from Figs. 4 and 8. This finding may just highlight the obvious point that the more a galaxy accretes gas the more stars it forms. However, the regularity of this link seems to point at a more fundamental interplay between star formation and accretion (see also the discussion in Hopkins et al. 2008). In a series of papers (Fraternali & Binney 2008; Marinacci et al. 2010, 2011) it has been suggested that gas accretion in discs is fundamentally related to star formation because it is produced by supernova (*positive*) feedback. Supernovae eject (high-metallicity) gas clouds out of galactic discs mixing it with the surrounding hot corona and causing prompt cooling of the latter. This implies an accretion that follows closely the star formation in the disc and proceeds from inside out given the distribution of cloud orbits (Fraternali & Binney 2006). Marasco et al. (2011) applied this model to the Milky Way and found a global accretion rate of $\sim 2 M_{\odot} \text{yr}^{-1}$. They also found that the current accretion profile is an increasing function of the radius out to a peak at $R \sim 9 \text{ kpc}$ followed by a sudden drop further out. In this paper, we found a similar shape but with a peak located closer in, see Fig. 6. How-

ever, as mentioned, our approach traces the location where the new gas forms stars. So it is conceivable that the infall took place at slightly larger radii, and then it flowed quiescently in. It is compelling that two completely independent methods as these produce such similar accretion patterns and global gas accretion rates.

5 CONCLUSIONS

In this paper we have proposed a simple method to derive the amount of gas needed for the star formation to proceed in a galactic disc, using the Kennicutt-Schmidt law. We found that in typical disc galaxies (Sb or later types) most star-forming gas is not in place in the disc at the time of formation but needs to be slowly acquired from the surrounding environment. We derived the gas accretion rate as a function of time for the Milky Way and other 21 disc galaxies from the THINGS sample. We parametrized the SFH with a simple polynomial function with a parameter (γ) that defines the slope of the SFH, $\gamma = 1$ stands for a flat SFH. We summarize our results as follows:

- (i) the disc of the Milky Way as a whole (not only the Solar neighborhood) formed stars in the past a rate that was $\sim 2 - 3$ times larger than now;
- (ii) the steepness of the SFH is a function of galaxy mass and Hubble type, with late type galaxies having nearly flat or inverted SFH;
- (iii) gas accretion is tightly linked to star formation, a constant ratio between the two is maintained for a large fraction of the life of a galaxy, pointing at a reciprocal interplay;
- (iv) galaxy discs must have experienced accretion of large fraction of their mass (in gaseous form) after $z = 1$, unless the K-S law had a strong evolution with z ;
- (v) gas accretion progressively moves from the inner to the outer regions of galaxy discs, as a consequence star formation also proceeds inside-out;
- (vi) the efficiency of gas accretion is less than 1 and decreases with time in all galaxies except some late-type dwarfs, as a consequence the gas consumed by star formation is not completely replenished and the galaxy eventually stops forming stars;
- (vii) the present-time accretion rates we derive are very uncertain, but even so there are indications that some large spirals may not need ongoing gas accretion.

An obvious development of this study would be to incorporate metallicity. Our results on the amount of gas infall needed for the Galaxy are broadly in agreement with the amount of infalling material needed by chemical evolution models. Our independent determination of the infall rate as a function of time and radius could be taken as an input in chemical evolution models to obtain a better understanding of the accretion mechanisms that feed the star formation in galaxy discs.

ACKNOWLEDGMENTS

We thank Andrew Hopkins and Donatella Romano for very helpful advice and stimulating discussions. We are grateful to an anonymous referee for helpful and constructive

comments. FF was supported by the PRIN-MIUR 2008SP-TACC. MT was supported for this research through a stipend from the International Max Planck Research School (IMPRS) for Astronomy and Astrophysics at the Universities of Bonn and Cologne, and by the SFB 956 "Conditions and Impact of Star Formation" by the Deutsche Forschungsgemeinschaft (DFG).

REFERENCES

- Aumer M., Binney J. J., 2009, *MNRAS*, 397, 1286
- Bauermeister A., Blitz L., Ma C., 2010, *ApJ*, 717, 323
- Bell E. F., McIntosh D. H., Katz N., Weinberg M. D., 2003, *ApJS*, 149, 289
- Bigiel F., Leroy A., Walter F., Brinks E., de Blok W. J. G., Madore B., Thornley M. D., 2008, *AJ*, 136, 2846
- Binney J., Dehnen W., Bertelli G., 2000, *MNRAS*, 318, 658
- Binney J., Merrifield M., 1998, *Galactic Astronomy*. Princeton University Press
- Binney J., Nipoti C., Fraternali F., 2009, *MNRAS*, 397, 1804
- Binney J., Tremaine S., 2008, *Galactic Dynamics: Second Edition*. Princeton University Press
- Bland-Hawthorn J., 2009, in J. Andersen, J. Bland-Hawthorn, & B. Nordström ed., *IAU Symposium Vol. 254 of IAU Symposium, Warm gas accretion onto the Galaxy*. pp 241–254
- Boissier S., Prantzos N., 1999, *MNRAS*, 307, 857
- Boissier S., Prantzos N., Boselli A., Gavazzi G., 2003, *MNRAS*, 346, 1215
- Brinchmann J., Charlot S., White S. D. M., Tremonti C., Kauffmann G., Heckman T., Brinkmann J., 2004, *MNRAS*, 351, 1151
- Cappellari M., Emsellem E., Krajnović D., McDermid R. M., Serra P., Alatalo K., Blitz L., Bois M., Bournaud F., Bureau M., Davies R. L., Davis T. A., de Zeeuw P. T., Khochfar S., Kuntschner H., Lablanche P.-Y., 2011, *MNRAS*, 416, 1680
- Case G. L., Bhattacharya D., 1998, *ApJ*, 504, 761
- Chabrier G., 2003, *PASP*, 115, 763
- Chiappini C., Matteucci F., Gratton R., 1997, *ApJ*, 477, 765
- Chiappini C., Matteucci F., Romano D., 2001, *ApJ*, 554, 1044
- Cignoni M., Degl’Innocenti S., Prada Moroni P. G., Shore S. N., 2006, *A&A*, 459, 783
- Collins J. A., Shull J. M., Giroux M. L., 2009, *ApJ*, 705, 962
- Dehnen W., Binney J., 1998, *MNRAS*, 294, 429
- Dekel A., Birnboim Y., 2006, *MNRAS*, 368, 2
- Diehl R., Halloin H., Kretschmer K., Lichti G. G., Schönfelder V., Strong A. W., von Kienlin A., Wang W., Jean P., Knödseder J., Roques J., Weidenspointner G., Schanne S., Hartmann D. H., Winkler C., Wunderer C., 2006, *Nature*, 439, 45
- Fraternali F., 2009, in J. Andersen, J. Bland-Hawthorn, & B. Nordström ed., *IAU Symposium Vol. 254 of IAU Symposium, New evidence for halo gas accretion onto disk galaxies*. pp 255–262
- Fraternali F., Binney J. J., 2006, *MNRAS*, 366, 449
- Fraternali F., Binney J. J., 2008, *MNRAS*, 386, 935
- Gogarten S. M., Dalcanton J. J., Williams B. F., 2009, in *The Evolving ISM in the Milky Way and Nearby Galaxies The Spatially Resolved Star Formation History of NGC 300*
- Harris J., Zaritsky D., 2009, *AJ*, 138, 1243
- Haywood M., 2001, *MNRAS*, 325, 1365
- Hopkins A. M., Beacom J. F., 2006, *ApJ*, 651, 142
- Hopkins A. M., Irwin M. J., Connolly A. J., 2001, *ApJL*, 558, L31
- Hopkins A. M., McClure-Griffiths N. M., Gaensler B. M., 2008, *ApJL*, 682, L13
- Jorgenson R. A., Wolfe A. M., Prochaska J. X., Carswell R. F., 2009, *ApJ*, 704, 247
- Joung M. R., Bryan G. L., Putman M. E., 2011, *ArXiv e-prints*
- Kalberla P. M. W., Dedes L., 2008, *A&A*, 487, 951
- Kaufmann T., Bullock J. S., Maller A. H., Fang T., Wadsley J., 2009, *MNRAS*, 396, 191
- Kaufmann T., Mayer L., Wadsley J., Stadel J., Moore B., 2006, *MNRAS*, 370, 1612
- Kennicutt Jr. R. C., 1983, *ApJ*, 272, 54
- Kennicutt Jr. R. C., 1998a, *ARA&A*, 36, 189
- Kennicutt Jr. R. C., 1998b, *ApJ*, 498, 541
- Kennicutt Jr. R. C., Calzetti D., Walter F., Helou G., Hollenbach D. J., Armus L., Bendo G., Dale D. A., Draine B. T., Engelbracht C. W., Gordon K. D., Prescott M. K. M., W. R. M., Thornley M. D., Bot C., Brinks E., de Blok E., et al. 2007, *ApJ*, 671, 333
- Kennicutt Jr. R. C., Tamblyn P., Congdon C. E., 1994, *ApJ*, 435, 22
- Kroupa P., Tout C. A., Gilmore G., 1993, *MNRAS*, 262, 545
- Krumholz M. R., Dekel A., 2011, *ArXiv e-prints*
- Krumholz M. R., Dekel A., McKee C. F., 2012, *ApJ*, 745, 69
- Krumholz M. R., Leroy A. K., McKee C. F., 2011, *ApJ*, 731, 25
- Lah P., Chengalur J. N., Briggs F. H., Colless M., de Propris R., Pracy M. B., de Blok W. J. G., Fujita S. S., Ajiki M., Shioya Y., Nagao T., Murayama T., Taniguchi Y., Yagi M., Okamura S., 2007, *MNRAS*, 376, 1357
- Lehner N., Howk J. C., 2011, *Science*, 334, 955
- Leroy A. K., Walter F., Brinks E., Bigiel F., de Blok W. J. G., Madore B., Thornley M. D., 2008, *AJ*, 136, 2782
- Lyne A. G., Manchester R. N., Taylor J. H., 1985, *MNRAS*, 213, 613
- Maeder A., Meynet G., 1989, *A&A*, 210, 155
- Maller A. H., Bullock J. S., 2004, *MNRAS*, 355, 694
- Marasco A., Fraternali F., Binney J. J., 2011, *ArXiv e-prints*
- Marinacci F., Binney J., Fraternali F., Nipoti C., Ciotti L., Londrillo P., 2010, *MNRAS*, 404, 1464
- Marinacci F., Fraternali F., Nipoti C., Binney J., Ciotti L., Londrillo P., 2011, *MNRAS*, 415, 1534
- Matteucci F., Romano D., Molaro P., 1999, *A&A*, 341, 458
- Matteucci, F. ed. 2001, *The chemical evolution of the Galaxy Vol. 253 of Astrophysics and Space Science Library*
- Minchev I., Famaey B., Combes F., Di Matteo P., Mouhcine M., Wozniak H., 2011, *A&A*, 527, A147
- Murray N., Rahman M., 2010, *ApJ*, 709, 424

- Naab T., Ostriker J. P., 2006, MNRAS, 366, 899
- Nakanishi H., Sofue Y., 2006, PASJ, 58, 847
- Nipoti C., 2010, MNRAS, 406, 247
- Pagel B. E. J., Patchett B. E., 1975, MNRAS, 172, 13
- Panter B., Jimenez R., Heavens A. F., Charlot S., 2007, MNRAS, 378, 1550
- Peek J. E. G., 2009, ApJ, 698, 1429
- Peek J. E. G., Putman M. E., Sommer-Larsen J., 2008, ApJ, 674, 227
- Piontek F., Steinmetz M., 2011, MNRAS, 410, 2625
- Prantzos N., 2008, in Charbonnel C., Zahn J.-P., eds, EAS Publications Series Vol. 32 of EAS Publications Series, An Introduction to Galactic Chemical Evolution. Cambridge University Press, pp 311–356
- Rocha-Pinto H. J., Scalo J., Maciel W. J., Flynn C., 2000, A&A, 358, 869
- Roškar R., Debattista V. P., Quinn T. R., Stinson G. S., Wadsley J., 2008, ApJL, 684, L79
- Roychowdhury S., Chengalur J. N., Begum A., Karachentsev I. D., 2009, MNRAS, 397, 1435
- Sancisi R., Fraternali F., Oosterloo T., van der Hulst T., 2008, A&ARv, 15, 189
- Scalo J. M., 1986, Fundamentals of Cosmic Physics, 11, 1
- Schaye J., 2004, ApJ, 609, 667
- Schmidt M., 1959, ApJ, 129, 243
- Searle L., Sargent W. L. W., 1972, Comments on Astrophysics and Space Physics, 4, 59
- Sellwood J. A., Binney J. J., 2002, MNRAS, 336, 785
- Thom C., Peek J. E. G., Putman M. E., Heiles C., Peek K. M. G., Wilhelm R., 2008, ApJ, 684, 364
- Tinsley B. M., 1980, Fundamentals of Cosmic Physics, 5, 287
- Tinsley B. M., Larson R. B., 1978, ApJ, 221, 554
- Tosi M., 1988a, A&A, 197, 33
- Tosi M., 1988b, A&A, 197, 47
- Twarog B. A., 1980, ApJ, 242, 242
- van de Voort F., Schaye J., Booth C. M., Dalla Vecchia C., 2011, MNRAS, 415, 2782
- Vincoletto L., Matteucci F., Calura F., Silva L., Granato G., 2012, MNRAS, 421, 3116
- Walter F., Brinks E., de Blok W. J. G., Bigiel F., Kennicutt Jr. R. C., Thornley M. D., Leroy A., 2008, AJ, 136, 2563
- Weisz D. R., Dalcanton J. J., Williams B. F., Gilbert K. M., Skillman E. D., Seth A. C., Dolphin A. E., McQuinn K. B. W., Gogarten S. M., Holtzman J., Rosema K., Cole A., Karachentsev I. D., Zaritsky D., 2011, ArXiv e-prints
- Wyder T. K., Martin D. C., Barlow T. A., Foster K., Friedman P. G., Morrissey P., Neff S. G., Neill J. D., Schiminovich D., Seibert M., Bianchi L., Donas J., Heckman T. M., Lee Y.-W., Madore B. F., Milliard B., Rich R. M., Szalay A. S., Yi S. K., 2009, ApJ, 696, 1834
- Zwaan M. A., van der Hulst J. M., Briggs F. H., Verheijen M. A. W., Ryan-Weber E. V., 2005, MNRAS, 364, 1467